Pre-Clinical Research Report

Journal of INTERNATIONAL MEDICAL RESEARCH

Journal of International Medical Research
2018, Vol. 46(6) 2359–2370

DOI: 10.1177/0300060518761787
journals.sagepub.com/home/imr
SAGE

Therapy of cervical cancer using ^{131}I-labeled nanoparticles

Wei Li[1,#], Danyang Sun[2,#], Ning Li[1], Yiming Shen[1], Yiming Hu[1] and Jian Tan[1]

Abstract

Objective: To evaluate the effectiveness of two kinds of Arg-Gly-Asp (RGD)-targeted ^{131}I-containing nanoliposomes for the treatment of cervical cancer *in vitro* and *in vivo*.

Methods: The nanoparticle liposomes designated RGD-^{131}I-tyrosine peptide chain (TPC)-L and ^{131}I-RGD-L were prepared. The emulsion solvent evaporation method was used to encapsulate the polypeptide into liposomes. The quantity of entrapped polypeptide was measured using UV spectrophotometry. The labeling rates, radiochemical purities, and total radioactivities were measured using paper chromatography. Cytotoxicity was assessed using the MTS assay and flow cytometry. Therapeutic efficacy was monitored using a mouse xenograft model of cervical cancer.

Results: The labeling efficiency, radiochemical purity, and specific radioactivity of RGD-^{131}I-TPC-L were greater than those of ^{131}I-RGD-L. The cytotoxicity test indicated that late apoptosis of cells treated with RGD-^{131}I-TPC-L and ^{131}I-RGD-L was higher than that of cells treated with Na^{131}I. The therapeutic effect of RGD-^{131}I-TPC-L was better than that of ^{31}I-RGD-L in the mouse model.

Conclusions: The specific activity of liposome-encapsulated RGD-^{131}I-TPC-L was higher than that of ^{131}I-RGD-L, which labeled liposomes directly. Moreover, the RGD-^{131}I-TPC-L liposomes were more effective for killing xenografted tumor cells.

Keywords

Liposome, polypeptide, radioiodine therapy, cervical cancer, Arg-Gly-Asp, nanoparticles

Date received: 6 October 2017; accepted: 6 February 2018

[1]Department of Nuclear Medicine, Tianjin Medical University General Hospital, Tianjin, PR China
[2]Department of Nuclear Medicine, Tianjin Medical University General Hospital Airport Hospital, Tianjin, PR China

[#]These authors contributed equally to this work.

Corresponding author:
Wei Li, Department of Nuclear Medicine, Tianjin Medical University General Hospital, Anshan Road 154, Heping district, Tianjin 300052, PR China.
Email: weiwei_tianjin@foxmail.com

Introduction

Cervical cancer is one of the most common cancers,[1] with a global incidence of 11.7% and an incidence of 13.4% in Chinese women.[2] The frequencies of cervical cancer are increasing, particularly for younger women.[3,4] The 5-year survival rates of patients with stage IV cervical cancer range from 20% to 30%, and the long-term rate of tumor recurrence is less than 30%.[5,6] There is special emphasis on how to select a treatment strategy to improve the quality of life of cancer survivors. ^{131}I emits high-energy X-rays and serves as an internal radiotherapeutic agent that can induce the killing of thyroid cancer cells by damaging their DNA through the effects of ionizing radiation.[7] ^{131}I inhibits the growth of cervical cancer-derived HeLa cells, and although ^{131}I only binds to the surface of thyroid cells, it cannot be internalized into other cancer cells that do not express sodium/iodide symporters.[8]

The development of nanomedicine provides a promising approach for enhancing drug delivery. The targeting of radionuclide-containing liposomes through internal radiotherapy is employed for imaging and treatment of tumor models using passive and active nanoparticle targeting to improve the biodistribution of pharmacological therapeutics.[9] The purpose of the present study was to analyze the differences in the therapeutic effects of ^{131}I incorporated into a tyrosine polypeptide chain (TPC) labeled with ^{131}I on tyrosine residues that was encapsulated into liposomes as well as the effects of liposomes directly labeled with ^{131}I.

Materials and methods

Materials

Liposome RGD-bovine serum albumin (BSA)-polycaprolactone (PCL) was synthesized and provided by Professor Chang Jin, Tianjin University.[10] Tyrosine peptide chain (TPC) and a peptide with a random sequence (random peptide chain [RPC]) were purchased from the Chinese Peptide Company (Hangzhou, China). The TPC and RPC sequences were YYYHYYK YYRYHYYYRYYHYYKY and HPLG SPGSASDLETSGLEEQR, respectively. ^{131}I-Na was purchased from the China Institute of Atomic Energy, Beijing, China.

Cell lines

The HeLa cervical cancer cell line was cultured in Dulbecco's Modified Eagle's medium supplemented with 10% fetal bovine serum (GIBCO Cell Culture [subsidiary of Invitrogen Corp.], Carlsbad, CA, USA), and 1% penicillin/streptomycin (Beijing Dongsheng Tebo Technology Company, Beijing, China). Cells were stored in a humidified atmosphere containing 5% CO_2 buffered with ambient air at 37 °C. The RGD peptide was overexpressed in HeLa cells.[11,12]

^{131}I labeling

The liposomes and TPC were labeled with ^{131}I using the chloramine-T method.[13] The ^{131}I-liposomes and ^{131}I-TPC were purified using centrifugal filtration (Amicon Pro Purification System, Merck Millipore, Billerica, MA, USA) to remove the remaining ^{131}I-Na. The dose of radioactivity, radiochemical purity, and the rates of incorporation of radioactivity into the products were determined using paper chromatography.[14] The developer was prepared using a 3:2:5 ratio of butyl alcohol:2 ethyl alcohol:5 ammonium hydroxide.

Preparation of ^{131}I-labeled liposomes

^{131}I-labeled liposomes were prepared as follows:[15] The RGD-targeting liposome encapsulating an RPC was directly labelled

with ^{131}I on the surface and named ^{131}I-RGD-L. The RGD-targeted liposomes that encapsulated ^{131}I-TPC were named RGD-^{131}I-TPC-L. The structures of radionuclide nanoparticles are shown in Figure 1a-1b. The emulsion solvent evaporation method was performed to encapsulate TPC or RPC into liposomes. The procedure was as follows: 2 mg of liposomes were dissolved in 2 mL of deionized water and then 300 μL of trioxymethylene solution was added. Immediately after the trioxymethylene and liposomes were sonicated (SCIENTZ-IID; Xin Zhi Biotechnology Co., Ltd., Zhejiang, China), the mixture was vibrated and centrifuged. The quantity of bound polypeptide was measured using a UV-visible spectrometer (UV-2450; Shimadzu Corporation, Beijing, China) at 220 nm.

Cellular uptake of ^{131}I

The RGD-BSA-PCL liposome was labeled with fluorescein isothiocyanate (FITC),[10] which can be easily imaged using confocal laser scanning microscopy (CLSM). The cellular uptake, targeting, and therapeutic effects of RGD-BSA-PCL are published.[16] CLSM was used to evaluate the uptake by HeLa cells of FITC-labeled liposomes that encapsulated TPC or RPC.

Cellular uptake of ^{131}I-RGD-L and RGD-^{131}I-TPC-L

Cervical cancer-derived HeLa cells were seeded in 6-well plates and cultured with 1.85 MBq/mL of radioactive nanoliposomes.[16] Cells were washed, lysed, centrifuged, and counted at different times. Radioactivity was measured using a γ-counter (LKB Gamma Counter 1261; LKB Instruments, Mount Waverley, Australia). All of experiments were performed in triplicate.

Apoptosis assays

The MTS assay was conducted according to a published procedure[17] to calculate the half-maximal inhibitory concentration (IC_{50}) of 131-labelled liposomes after 24 hours.[18] Flow cytometry was performed according to the IC_{50} value. HeLa cells were seeded into a 6-well plate and incubated with 18.7 MBq/mL of RGD-^{131}I-L, RGD-^{131}I-TPC-L, or Na^{131}I for 24 hours, washed twice, lysed, and centrifuged. The cells were then incubated with FITC-Annexin-V and propidium iodide. Flow cytometric analysis (BD Biosciences, San Jose, CA, USA) was performed.

Mouse model

BALB/c mice (female, aged 4–5 weeks, 15 to 20 g) were purchased from the Beijing Experimental Animal Center of Peking Union Medical, China. Mice were kept under specific pathogen-free conditions in the Laboratory Animal Center of Tianjin Medical University, China. All animal studies were conducted in accordance with a protocol approved by the Tianjin Medical University General Hospital Ethics Committee. The animal experiment guidelines were followed according to the regulations of Swiss veterinary law.

HeLa cells were subcutaneously injected into the right flank. When the tumor volume reached 0.7 cm in diameter, the mice were randomly divided into three groups of five mice each. According to the principles of the human thyroid perchlorate discharge test, 0.05 mg/mL sodium perchlorate was added to the drinking water of all mice 1 day before injection of the radionuclide.[19] The mice were killed when neurological symptoms appeared or a loss of 20% of original body weight.

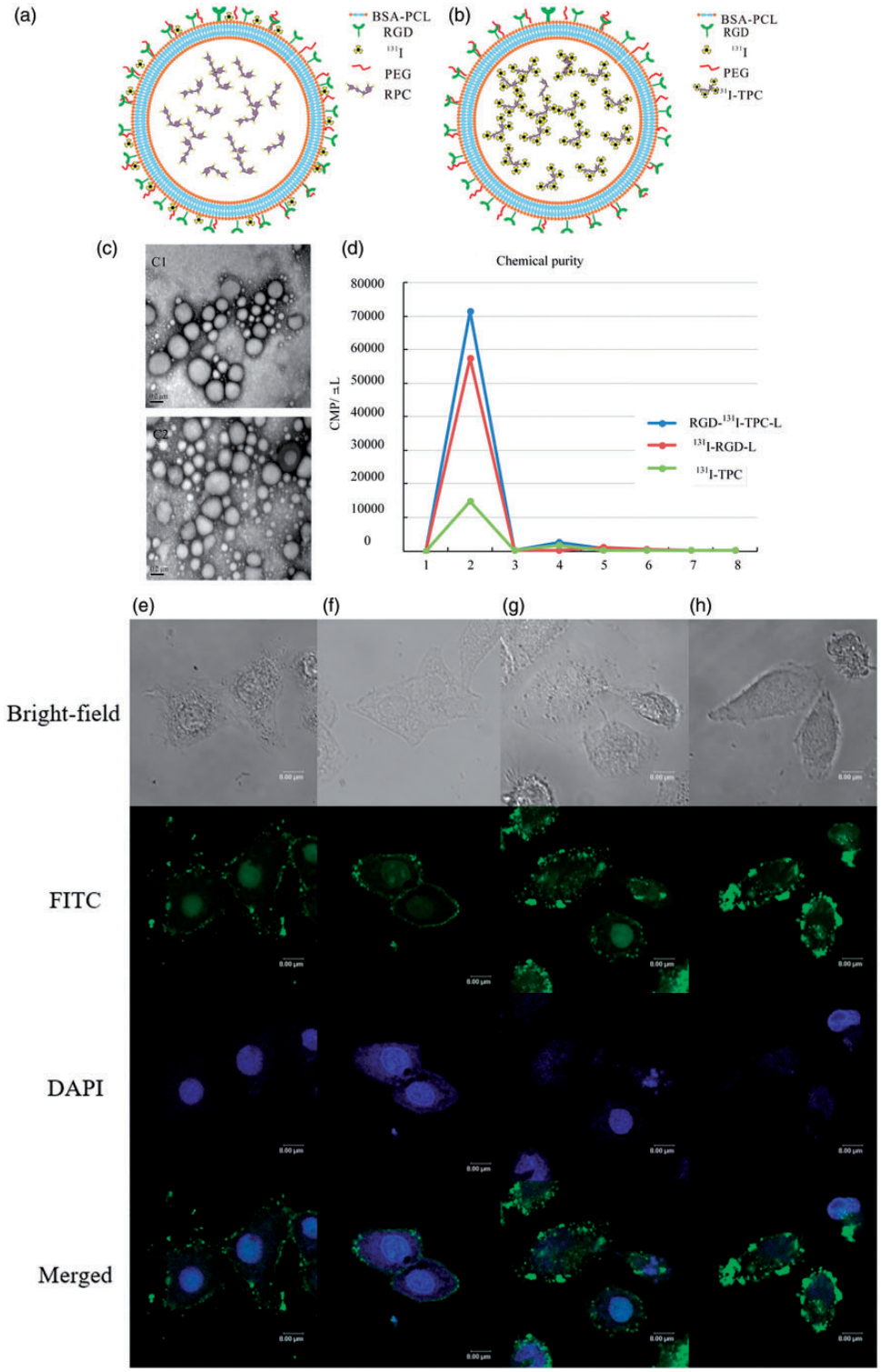

Figure 1. Characteristics of ^{131}I-labeled nanoparticles

Distribution of ^{131}I in mice

Mice were sacrificed at 24, 48, and 72 hours postinjection. Heart, spleen, liver, kidney, and tumor samples were collected for weighing, and radioactivity was measured using a γ-counter. The percentage injected dose (ID) per gram of tissue was calculated.[20]

Radioiodine therapy

When a tumor's diameter reached 0.7 cm, 74 MBq of ^{131}I-labeled liposomes, ^{131}I-Na, or an equivalent volume of normal saline was injected into the tumor. During treatment, the animal's body weight and in vivo tumor growth were measured. Body weights and tumor volumes (volume = $1/6 \times \pi \times$ length [cm] $\times$ width [cm] $\times$ height [cm]) were measured. Antitumor activity was evaluated by determining the relative tumor increase rate (T/C) as follows: T/C (%) = TRTV/CRTV x 100. Therapeutic efficiency was evaluated as follows: T/C >40% indicated no therapeutic effect, whereas T/C $\leq$40% ($P<0.05$) indicated a positive therapeutic effect. The tumor inhibition rate (TIR) was calculated by comparing the weights of the transplanted tumors of the treatment group with those of the negative control group as follows: TIR (%) = (1-mean weight of the transplanted tumor of the treatment group per mean weight of the transplanted tumor of the negative control group) $\times$ 100.[21] The therapy groups were followed for 30 days after injection and then killed.

SPECT/CT whole-body imaging of mice

To assess the organ localization of ^{131}I, single-photon computed tomography/computed tomography (SPECT/CT) (Discovery VH 670; GE, Chicago, IL, USA) was performed. Mice from the three treatment groups, except for the normal saline group, received an intratumor injection of 74 MBq (740 MBq/mL) of radioliposomes and Na^{131}I, respectively.[22]

Histopathology studies

When the radioiodine therapy experiment concluded, normal tissues including the heart, liver, spleen, and kidney were isolated. Sections were stained with hematoxylin and eosin for histopathological analyses. The histopathological changes of the tissue were examined using light microscopy, $\times$40 magnification (Olympus Th4-200; Olympus Optical Company, Beijing, China).

Statistical analysis

Statistical analysis was performed using IBM SPSS Statistics, version 22.0 (IBM Corp., Armonk, NY, USA). Data were evaluated using the Student t test or one-way ANOVA. The difference between the two groups was considered significant when the $P<0.05$ indicated a significant difference between two groups.

Figure 1. Continued.
A. I ^{131}I-RGD-L; B. RGD-^{131}I-TPC-L. The RGD-targeted liposomes encapsulating an RPC were directly labeled on the surface with Na^{131}I. B. RGD-targeted liposomes encapsulating the ^{131}I-TPC. C. Dynamic light scattering determinations of the diameters of RGD-TPC-L (C1) and RGD-L(C2). D. The radiochemical purities of ^{131}I-TPC, RGD-^{131}I-TPC-L and ^{131}I-RGD-L. E. Liposome encapsulated TPC at 2 hours; F. Liposome encapsulated RPC at 2 hours; G. Liposome encapsulated TPC at 6 hours; H. Liposome encapsulated RPC at 6 hours. Scale bars = 20 μm. The green fluorescence intensities of L-TPC and L-RPC were similar when measured at 2 hours and 6 hours in HeLa cells. 4',6-diamidino-2-phenylindole nuclear staining is shown in blue. Abbreviations: RGD, Arg-Gly-Asp; TPC, tyrosine peptide chain, RPC, random peptide chain.

Results

Characteristics of nanoparticles

Dynamic light scattering measurements showed that the diameters of RGD-TPC-L and RGD-L were not significantly different (264.7 ± 17.6 nm and 275.4 ± 18.7 nm, respectively) (Figure 1c). The polydispersity index was 0.17, and the zeta potential was −41.30 mV.

Encapsulation of TPC and RPC into liposomes

The amounts of TPC or RPC encapsulated into liposomes using 100 μg, 200 μg, 300 μg, 500 μg, and 1000 μg of starting material were not significantly different. Their respective amounts (μg) encapsulated into liposomes were as follows: 75.9 ± 10.91 vs 69.1 ± 12.88, 123.7 ± 25.1 vs 133.2 ± 34.5, 158.9 ± 33.94 vs 146.7 ± 36.2, 192.8 ± 31.3 vs 189.0 ± 41.26, and 219.6 ± 51.4 μg vs 234.7 ± 45.87, respectively. UV spectroscopy showed that the amount of each encapsulated polypeptide was 500 μg.

^{131}I-labeling

The maximum yields of radioactivities of 1 mg of liposomes labeled with ^{131}I-RGD-L and RGD-^{131}I-TPC-L were 170.2 ± 50.3 MBq and 699.3 ± 79.6 MBq, respectively ($P<0.05$). The efficiencies of labeling RGD-^{131}I-TPC-L and ^{131}I-RGD-L were $85.7 \pm 7.4\%$ vs $72.5 \pm 9.8\%$, respectively ($P<0.05$). The radiochemical purities of ^{131}I-TPC, RGD-^{131}I-TPC-L and ^{131}I-RGD-L were not significantly different ($96.5 \pm 1.9\%$, $92.0 \pm 2.6\%$, and $94.8 \pm 1.7\%$, respectively (Figure 1d).

Internalization of liposome-encapsulated polypeptides

Confocal microscopy was used to evaluate the internalization of liposomes in HeLa cells. Liposomes encapsulating TPC and RPC were significantly internalized in HeLa cells and exhibited strong green fluorescence (Figure 1e–h). The fluorescence intensities of FITC-L-TPC and FITC-L-RPC were similar after incubation with HeLa cells for 2 hours and 6 hours.

Intracellular retention of ^{131}I

The retention times of ^{131}I by nuclear liposomes in HeLa cells are shown in Figure 2a. RGD-^{131}I-TPC-L and ^{131}I-RGD-L exhibited increased intracellular retention, which reached maximum levels at 6 hours. The CPM/10^5 cells of RGD-^{131}I-TPC-L and ^{131}I-RGD-L were $138\,763.6 \pm 7421.9$ vs $125\,692.1 \pm 9\,430.3$, respectively. However, the radioactivity of the Na^{131}I group was relatively low.

Apoptosis assay

The MTS assay determined that the IC_{50} values of ^{131}I- RGD-L and RGD-^{131}I-TPC-L were approximately 1.85 MBq/mL. The rates of late apoptosis measured using flow cytometry (Annexin V+/PI+) of HeLa cells incubated with ^{131}I-RGD-L, RGD-^{131}I-TPC-L, and Na^{131}I were $10.3 \pm 0.67\%$, $11.9 \pm 0.46\%$, and $5.1 \pm 0.38\%$, respectively ($P<0.05$) (Figure 2d–2f). RGD-^{131}I-TPC-L and ^{131}I-RGD-L were more cytotoxic than Na^{131}I and normal saline. There was not a significant difference between the cytotoxicities of RGD-^{131}I-TPC- L and ^{131}I-RGD-L.

Biodistribution analysis

Comparisons of the biodistribution data of RGD-^{131}I-TPC-L, ^{131}I-RGD-L and Na^{131}I in the tumor and normal tissues of mice were measured according to γ-counts. The uptake values of RGD-^{131}I-TPC-L, ^{131}I-RGD-L 24, 48, and 72 hours postinjection were $25.7 \pm 5.13\%$ ID/g, $17.4 \pm 3.43\%$ ID/g, $8.7 \pm 2.64\%$ ID/g versus 19.7

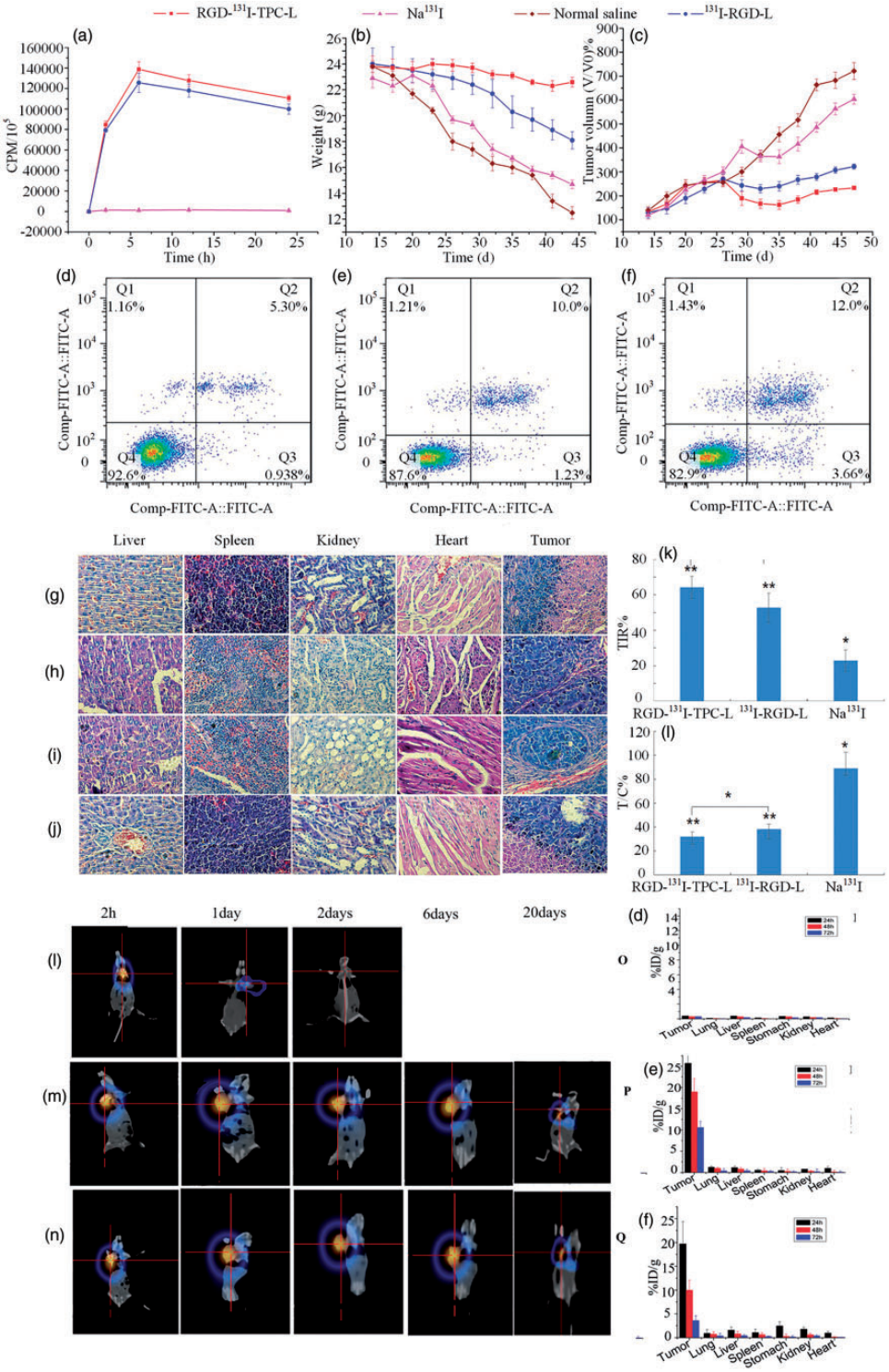

Figure 2. The characteristics and treatment of ^{131}I-labeled nanoparticles

$\pm 4.66\%$ ID/g, $9.9 \pm 2.11\%$ ID/g, and $3.6 \pm 1.03\%$ ID/g, respectively, and were significantly higher compared with those of the $Na^{131}I$ group ($0.41 \pm 0.12\%$ ID/g, $0.31 \pm 0.08\%$ ID/g, $0.29 \pm 0.10\%$ ID/g (Figure 2g–2j). However, the uptake of all radionuclides was low and differed slightly among organs such as the heart, liver, spleen, and kidneys at all times.

Radiotherapy

The differences between *in vivo* and *in vitro* experiments required further evaluation of radioactive iodine treatment of cervical cancer using two types of nuclear liposomes. Therefore, a mouse xenograft model of cervical cancer was established. The average tumor volumes of the RGD-^{131}I-TPC-L and ^{131}I-RGD-L groups were smaller compared with those of the $Na^{131}I$ and normal saline groups (Figure 2b, 2c). The tumor volumes of the RGD-^{131}I-TPC-L, ^{131}I-RGD-L groups were significantly reduced compared with that of the $Na^{131}I$ or normal saline groups. On day 15, compared with the other groups, RGD-^{131}I-TPC-L exhibited improved tumor inhibition, and the differences in the declining values of the T/C were significant ($P < 0.01$) (Figure 2l).

Figure 2. Continued.
A. RGD-^{131}I-TPC-L and ^{131}I-RGD-L exhibited increased retention of ^{131}I, and the intracellular level of ^{131}I reached its maximum at 6 hours. The radioactivity of the $Na^{131}I$ group was maintained at a low level. B. Weights of mice with tumors injected with RGD-^{131}I-TPC-L, ^{131}I-RGD-L, $Na^{131}I$, and normal saline. The weights of the ^{131}I and the normal saline group decreased; however, the weights of the RGD-^{131}I-TPC-L and ^{131}I-RGD-L groups did not differ significantly during the course of ^{131}I therapy. C. The $Na^{131}I$ and the normal saline groups showed sustained growth, in contrast to the decreased growth of the RGD-^{131}I-TPC-L and ^{131}I-RGD-L groups. D–F. Apoptosis assays. D. $Na^{131}I$; E. ^{131}I-RGD-L; F. RGD-^{131}I-TPC-L. RGD-^{131}I-TPC-L and ^{131}I-RGD-L induced increased apoptosis compared with the $Na^{131}I$ groups. The extents of late apoptosis induced by $Na^{131}I$, ^{131}I-RGD-L, and RGD-^{131}I-TPC-L were $10.3 \pm 0.67\%$, $11.9 \pm 0.46\%$ and $5.1 \pm 0.38\%$, respectively. G–J. G. RGD-^{131}I-TPC-L; H. Normal saline; I. $Na^{131}I$; J. ^{131}I-RGD-L. The potential toxicity of liposomes was investigated using hematoxylin and eosin staining. No significant pathological changes in the heart, liver, spleen, and kidneys were observed in nude mice following treatment with RGD-L-^{131}I-TPC, ^{131}I -RGD-L, $Na^{131}I$, and normal saline. Images were acquired at a magnification of 40×. K. The T/C % of the treatment groups. The T/C values of the RGD-^{131}I-TPC-L and ^{131}I-RGD-L treatment groups were greatly reduced, with a significant reduction compared with the normal control (NC) group. The T/C of the $Na^{131}I$ group was >40%, and the decline in the T/C values of the RGD-^{131}I-TPC-L and ^{131}I-RGD-L differed significantly (*$P<0.05$, **$P<0.01$). L. The TIR% of the treatment groups. The TIR values of the RGD-^{131}I-TPC-L and ^{131}I-RGD-L treatment groups were significantly higher compared with those of the $Na^{131}I$ and NC groups. The TIR of the RGD-^{131}I-TPC-L group was significantly higher compared with that of the ^{131}I-RGD-L group (*$P<0.05$, **$P<0.01$). L–N. SPECT/CT images. L. $Na^{131}I$; M. RGD-^{131}I-TPC-L; N. ^{131}I-RGD-L. Nanoliposomes or ^{131}I were injected into xenografted tumors, and images were acquired at different times using SPECT/CT (74 MBq per mouse, $n = 5$). The xenografted tumors of the $Na^{131}I$ group emitted weak signals on the day of injection, and subsequently there was little uptake of ^{131}I uptake in the xenografted tumor. However, SPECT/CT imaging revealed that the tumor retained had RGD-L -^{131}I-TPC and ^{131}I -RGD-L for 20 days. The tumor area exhibited higher accumulations and significantly longer residence times in the RGD-L-^{131}I -TPC and ^{131}I -RGD-L groups compared those of the ^{131}I groups. O–Q. The Biodistribution of radionuclide nanoparticles. O. $Na^{131}I$; P. ^{131}I-RGD- L; Q. RGD-^{131}I-TPC-L. the biodistribution of RGD-^{131}I-TPC-L, ^{131}I-RGD-L, and $Na^{131}I$ in nude mice with tumors formed by xenografted HeLa cells 24, 48, and 72 hours after injection (74 MBq per mouse, $n = 5$). The levels of uptake of ^{131}I by the RGD-^{131}I-TPC-L and ^{131}I-RGD- L groups were significantly higher compared with that of the $Na^{131}I$ group, and the normal tissues accumulated low levels of radioactivity at all times in all three groups. The uptake of $Na^{131}I$ at all times was very low in normal and tumor tissues in the $Na^{131}I$ group. Abbreviation: SPECT/CT, single-photon computed tomography/computed tomography.

The TIR values of the RGD-^{131}I-TPC-L group were higher compared with those of the other groups, and the differences among these groups were significant ($P < 0.01$) (Figure 2k). These results show that RGD-^{131}I-TPC-L had the best therapeutic effects in our mouse model of cervical cancer.

Histopathological analysis

To test the potential toxicity of liposomes in experimental mice, hematoxylin and eosin–stained sections of the heart, liver, spleen, and kidneys were examined after radiotherapy. The histopathological images of the major organs are shown in Figure 2g–2j. Significant pathological changes in vital organs were not observed in nude mice following treatment using RGD-^{131}I-TPC-L, ^{131}I-RGD-L or Na^{131}I, indicating the limited toxicity of ^{131}I-labeled liposomes. Pathological examination revealed degeneration and necrosis of tumor cells in groups injected with RGD-^{131}I-TPC-L and ^{131}I-RGD-L.

SPECT/CT imaging

RGD-^{131}I-TPC-L, ^{131}I-RGD-L, and Na^{131}I were injected into the tumors. Representative SPECT/CT images are shown in Figure 2l–2n. The Na^{131}I group emitted a weak signal from the xenografted tumor on the day of injection. There was no significant subsequent uptake of ^{131}I uptake into the xenografted tumor (Figure 2l). In contrast, the RGD-^{131}I-TPC-L and ^{131}I-RGD-L groups had higher accumulations of ^{131}I in the region of the xenografted tumors compared with the Na^{131}I group. The levels of radioactivity emitted by RGD-^{131}I-TPC-L and ^{131}I-RGD-L were detectable 20 days after injection, indicating that the RGD-^{131}I-TPC-L and ^{131}I-RGD-L groups retained radioactivity significantly longer than the Na^{131}I group.

Discussion

Here we developed two different types of radioactive nanoparticle liposomes, designated RGD-^{131}I-TPC-L and ^{131}I-RGD-L, to analyze their therapeutic effects on cultured HeLa cells and in a mouse xenograft model of cervical cancer. Cyclic-RGD-conjugated liposomes are a desirable option for ligand delivery because of their improved bioavailability and enhanced receptor affinity, imparted by the multivalent peptide display effect.[23] ^{131}I is ideal for therapeutic use (gamma emission, 364 KeV [81.7%] and a beta emission, 0.606 MeV [89.9%]).

Strategies for labeling or encapsulating radiolabeled nanoparticles include labeling nanoparticles during their preparation, labeling the nanoparticle's surface after encapsulation, labeling bioconjugates bound to the nanoparticle's surface after encapsulation, incorporation into the lipid bilayer after encapsulation by liposomes, and after loading of the aqueous phase of the liposomes.[24] Here, we first explored the properties of ^{131}I-TPC encapsulated into liposomes via self-assembly using the emulsion solvent evaporation method. Previous *in vivo* biodistribution and pharmacokinetics studies ^{131}I used the standard chloramine-T oxidation method to conjugate ^{131}I to the surface of a nanoparticle.[25] Certain peptides can be encapsulated into nanoparticle liposomes, such as a peptide integrin antagonist, which are encapsulated in poly-lactic acid/oxidized plasma poly-lactic acid nanoparticles to increase the half-life of therapeutics.[26] Such studies indicate that the intracellular concentration of the peptide can be as high as its extracellular concentration without causing significant apoptosis. The peptide encapsulated into nanoparticles can significantly improve the specificity of delivery of a cancer chemotherapeutic drug and can mitigate

adverse side effects caused by off-target drug release.

Here we show that RGD-^{131}I-TPC-L delivered a higher dose of radioactivity and achieved better labeling rates than ^{131}I-RGD-L, because RGD-^{131}I-TPC-L encapsulated into liposomes incorporated more ^{131}I than ^{131}I-RGD-L. Thus, RGD-^{131}I-TPC-L was more cytotoxic than ^{131}I-RGD-L.

In our mouse model, a radionuclide liposome complex was injected into a xenografted tumor to bind to the specific corresponding antigens of the tumor cells. We used SPECT/CT imaging to monitor the characteristics of the radiotherapeutics in mice over time.[27] The RGD-^{131}I-TPC-L and ^{131}I-RGD-L groups had higher accumulations and longer sustained times in the tumor region compared with those of the Na^{131}I group, similar to the retention of ^{131}I by HeLa cells. In contrast, in the radiotherapy experiment, the RGD-^{131}I-TPC-L exhibited improved tumor inhibition and a decline of T/C compared with the ^{131}I-RGD-L and Na^{131}I groups. The results show that RGD-^{131}I-TPC-L had better therapeutic effects on cervical cancer, and may be explained as follows: 1) The amount of nanocarrier absorbed by tumor cells in nude mice was constant, and a unit of nanocarrier RGD-^{131}I-TPC-L bound more ^{131}I; 2) The cytotoxicities of radionuclide nanoparticles were not significantly different, because cytotoxicity was likely rapidly attenuated; 3) The effects of the ^{131}I-labeled nanoparticles differed in cultured HeLa cells vs tumors formed by xenografted HeLa cells.

RGD-L-^{131}I-TPC was labeled at a higher rate and to a higher specific activity per unit weight of liposomes compared with ^{131}I-RGD-L. This liposome RGD-^{131}I-TPC-L was more cytotoxic in the mouse xenograft model of cervical cancer, and few side effects were observed in the normal tissue compared with those of the other groups. Our method for encapsulating ^{131}I-TPC in liposomes may therefore represent an effective new method for treating cervical cancer.

Acknowledgements

We thank Professor Jin Chang, PhD for providing experimental materials, Zhongyun Liu, MD for advice, and and Lei Fang for secretarial assistance.

Declaration of conflicting interest

The authors declare that there is no conflict of interest

Funding

This research received no specific grant from any funding agency in the public, commercial, or not-for-profit sectors.

ORCID iD

Wei Li http://orcid.org/0000-0002-2035-0134

References

1. Torre LA, Bray F, Siegel RL, et al. Global cancer statistics, 2012. *CA Cancer J Clin* 2015; 65: 87–108.
2. Chen W, Zheng R, Zeng H, et al. The updated incidences and mortalities of major cancers in China, 2011. *Chin J Cancer* 2015; 34: 502–507.
3. Li S, Hu T, Lv WG, et al. Changes in prevalence and clinical characteristics of cervical cancer in the People's Republic of China: a study of 10,012 cases from a nationwide working group. *Oncologist* 2013; 18: 1101–1107.
4. Lertkhachonsuk AA, Yip CH, Khuhaprema T, et al. Cancer prevention in Asia: resource-stratified guidelines from the Asian Oncology Summit 2013. *Lancet Oncol* 2013; 14: E497–E507.
5. Quinn M, Benedet JL, Odicino F, et al. Carcinoma of the cervix uteri. *Int J Gynecol Obstet*. 2006; 95: S43–S103.
6. Rein DT, Kurbacher CM, Breidenbach M, et al. Weekly carboplatin and docetaxel for

locally advanced primary and recurrent cervical cancer: a phase I study. *Gynecol Oncol* 2002; 87: 98–103.
7. Huang P, Wu J, Li X, et al. RGD Peptide-Pegylated PLLA Nanoparticles containing Epirubicin Hydrochloride exhibit receptor-dependent tumor trafficking in Vitro and In Vivo. *Pharm Res* 2015; 32: 2328–2343.
8. Li W, Tan J, Wang P, et al. Glial fibrillary acidic protein promoters direct adenovirus early 1A gene and human telomerase reverse transcriptase promoters direct sodium iodide symporter expression for malignant glioma radioiodine therapy. *Mol Cell Biochem* 2015; 399: 279–289.
9. Allen TM and Cullis PR. Drug delivery systems: entering the mainstream. *Science* 2004; 303: 1818–1822.
10. Liu Z, Chen N, Dong C, et al. Facile Construction of Near Infrared Fluorescence Nanoprobe with Amphiphilic Protein-Polymer Bioconjugate for Targeted Cell Imaging. *ACS Appl Mater Interfaces* 2015; 7: 18997–19005.
11. Domingo-Espin J, Petegnief V, de Vera N, et al. RGD-based cell ligands for cell-targeted drug delivery act as potent trophic factors. *Nanomedicine*. 2012; 8: 1263–1266.
12. Mickler FM, Vachutinsky Y, Oba M, et al. Effect of integrin targeting and PEG shielding on polyplex micelle internalization studied by live-cell imaging. *J Control Release* 2011; 156: 364–373.
13. Nordberg E, Friedman M, Gostring L, et al. Cellular studies of binding, internalization and retention of a radiolabeled EGFR-binding affibody molecule. *Nucl Med Biol* 2007; 34: 609–618.
14. Mahlapuu M, Enerback S and Carlsson P. Haploinsufficiency of the forkhead gene Foxf1, a target for sonic hedgehog signaling, causes lung and foregut malformations. *Development* 2001; 128: 2397–2406.
15. Zambaux MF, Bonneaux F, Gref R, et al. Influence of experimental parameters on the characteristics of poly(lactic acid) nanoparticles prepared by a double emulsion method. *J Control Release* 1998; 50: 31–40.
16. Li W, Ji YH, Li CX, et al. Evaluation of therapeutic effectiveness of (131)I-antiEGFR-BSA-PCL in a mouse model of colorectal cancer. *World J Gastroenterol* 2016; 22: 3758–68.
17. Pedram S, Mohammadirad A, Rezvanfar MA, et al. On the protection by the combination of CeO2 Nanoparticles and Sodium Selenite on Human Lymphocytes against Chlorpyrifos-Induced Apoptosis In Vitro. *Cell J* 2015; 17: 361–371.
18. Zheng C, Ma C, Bai E, et al. Transferrin and cell-penetrating peptide dual-functioned liposome for targeted drug delivery to glioma. *Int J Clin Exp Med* 2015; 8: 1658–1668.
19. Lee YS, Bullard DE, Zalutsky MR, et al. Therapeutic efficacy of antiglioma mesenchymal extracellular matrix 131I-radiolabeled murine monoclonal antibody in a human glioma xenograft model. *Cancer Res*. 1988; 48: 559–566.
20. Li L, Wartchow CA, Danthi SN, et al. A novel antiangiogenesis therapy using an integrin antagonist or anti-Flk-1 antibody coated 90Y-labeled nanoparticles. *Int J Radiat Oncol Biol Phys* 2004; 58: 1215–1227.
21. Liu XY, Su X, Xie CJ, et al. Pharmacodynamic study of 131I-labeled CA215 antibody on an animal model of estrogen-resistant OC-3-VGH ovarian cancer. *Exp Ther Med* 2015; 10: 572–578.
22. Chang YJ, Chang CH, Chang TJ, et al. Biodistribution, pharmacokinetics and microSPECT/CT imaging of 188Re-bMEDA-liposome in a C26 murine colon carcinoma solid tumor animal model. *Anticancer Res*. 2007; 27: 2217–2225.
23. Hong S, Leroueil PR, Majoros IJ, et al. The binding avidity of a nanoparticle-based multivalent targeted drug delivery platform. *Chem Biol* 2007; 14: 107–115.
24. Ting G, Chang CH, Wang HE, et al. Nanotargeted radionuclides for cancer nuclear imaging and internal radiotherapy. *J Biomed Biotechnol* 2010; 2010.
25. Chen L, Zhong X, Yi X, et al. Radionuclide (131)I labeled reduced graphene oxide for nuclear imaging guided combined radio- and photothermal therapy of cancer. *Biomaterials* 2015; 66: 21–28.
26. Macho Fernandez E, Chang J, Fontaine J, et al. Activation of invariant Natural Killer T lymphocytes in response to the

alpha-galactosylceramide analogue KRN7000 encapsulated in PLGA-based nanoparticles and microparticles. *Int J Pharm* 2012; 423: 45–54.

27. Lee N, Puri DR, Blanco AI, et al. Intensity-modulated radiation therapy in head and neck cancers: an update. *Head Neck* 2007; 29: 387–400.